

Supporting Information

Controllable growth of WO₃@GDY heterointerface for efficient NH₃ synthesis

Determination of ammonia

Indophenol blue method was used for the detection of NH₃. Typically, 1 mL electrolyte (10-fold dilution of collected electrolyte) was mixed with 0.1 M NaOH, 125 µL color agent comprising 0.36 M salicylic acid, 0.36M NaOH, and 0.18M potassium sodium tartrate tetrahydrate, 12.5 µL 0.034M sodium nitroprusside and 12.5 µL NaClO/0.75 M NaOH solution. The UV-Vis measurements were performed after 1 h later and recorded with the range of 800 nm to 500 nm.

The ammonia concentration was determined by linear calibration curve of absorbance with serious known concentrations solution using the same indophenol blue method.

¹H NMR determination of ammonia

The synthesized ammonia was also determined by ¹H nuclear magnetic resonance (NMR, 400 MHz). Typically, 10 mg maleic acid was first dissolved into the 5 mL electrolytes, and the pH value was adjusted with 4 M H₂SO₄. Then 0.5 mL of the above solution was mixed with 0.05 mL DMSO-d₆ and tested by a 400 MHz SB Liquid Bruker Avance NMR spectrometer at room temperature.

Determination of nitrite

Griess reagent was used as the color-developing agent for the detection of NO₂⁻. Typically, the Griess reagent was composed of 0.8 g N-(1-Naphthyl) dihydrochloride, 0.04 g sulfanilamide, and 2 mL H₃PO₄ (85%) with 10 mL DI water. 2 mL electrolyte was mixed with 2 mL 0.1 M NaOH, after which mixed with the 40 µL Griess reagent and rested for 10 min at room temperature. UV-Vis spectrophotometer was used to record the absorption spectra in the range of 400-650 nm. And the nitrite concentration was determined by a linear calibration curve of absorbance with serious known concentrations solution using the same Griess test.

Calculation of FEs and Yield

The FE and yield of NH₃ were calculated as follows:

$$FE_{NH_3} = \frac{8 \times F \times C_{NH_4^+} \times V}{Q} \quad (\text{Equation 1})$$

$$Y_{NH_3} = \frac{C_{NH_4^+} \times V}{t \times S} \quad (\text{Equation 2})$$

where F is the Faradaic constant of 96485 C mol⁻¹, $C_{NH_4^+}$ (μg mL⁻¹) is the concentration of ammonia, V is the volume of the cathodic electrolyte (mL), Q (C) is the total charge passing the electrode, t (h) is the electrolysis time, S (cm²) is the area of the cathode.

The FE and yield of NO₂⁻ were calculated as follows:

$$FE_{NO_2^-} = \frac{2 \times F \times C_{NO_2^-} \times V}{Q} \quad (\text{Equation 3})$$

$$Y_{NO_2^-} = \frac{C_{NO_2^-} \times V}{t \times S} \quad (\text{Equation 4})$$

where F is the Faradaic constant of 96485 C mol⁻¹, $C_{NO_2^-}$ (μg mL⁻¹) is the concentration of ammonia which be calculated from the calibration curve, V is the volume of the cathodic electrolyte (mL), Q (C) is the total charge passing the electrode, t (h) is the electrolysis time, S (cm²) is the area of the cathode.

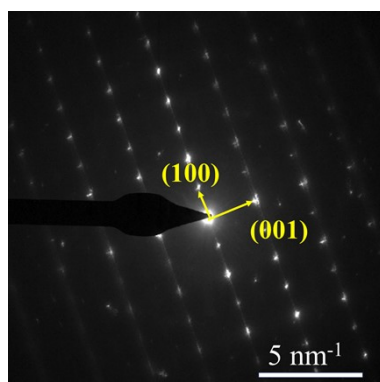


Figure S1. The SEAD pattern of WO₃@GDY.

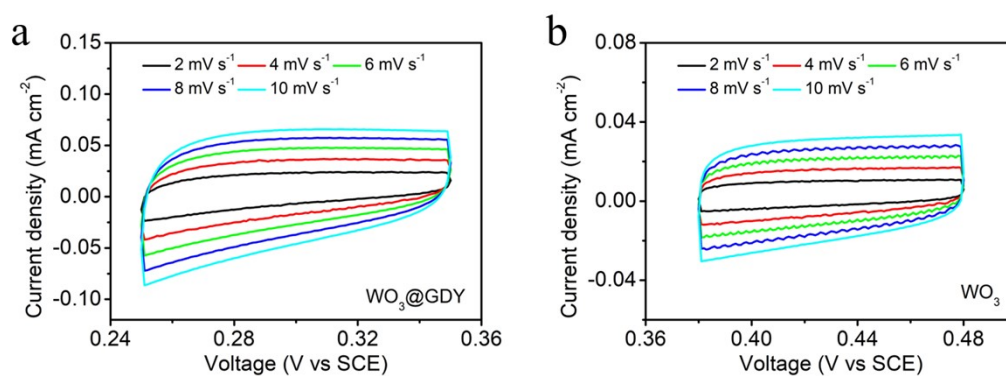


Figure S2 Cyclic voltammogram curves for a) WO₃@GDY, b) WO₃ catalysts at different scan rates.

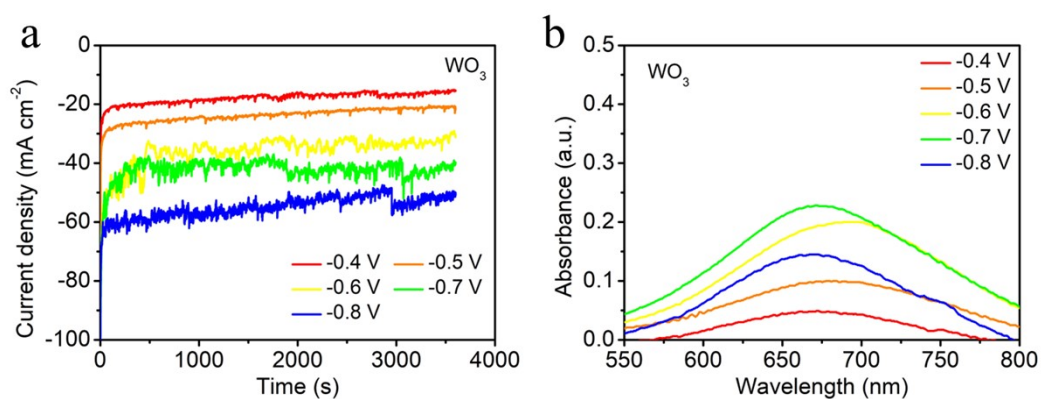


Figure S3. a) Chronoamperometry curves of WO₃ at different potentials. b) UV-Vis spectra of WO₃ with different voltages with diluted 10 times electrolyte.

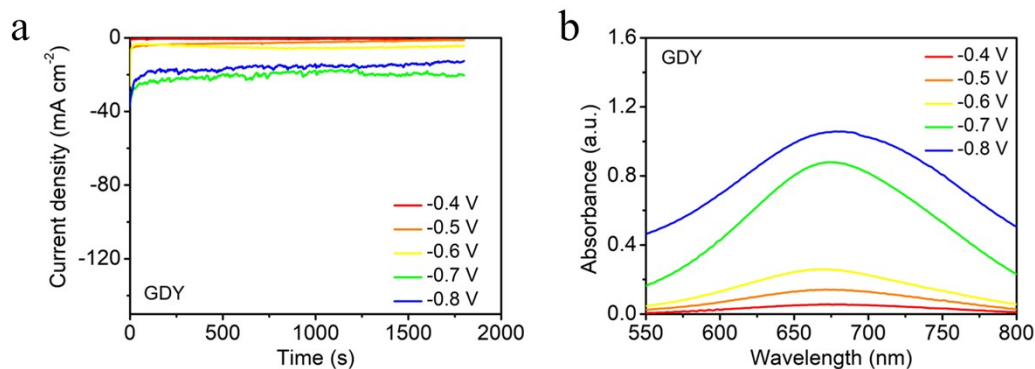


Figure S4. a) Chronoamperometry curves of GDY at different potentials. b) UV-Vis spectra of GDY with different voltages.

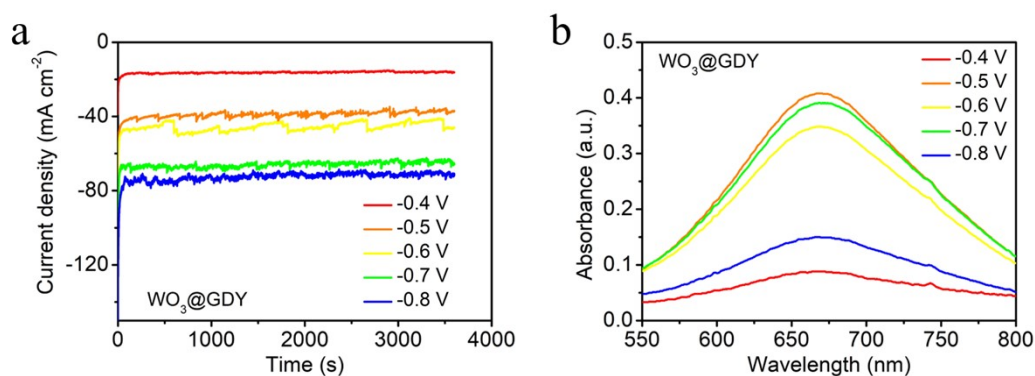


Figure S5. a) Chronoamperometry curves of WO₃@GDY at different potentials. b) UV-Vis spectra of WO₃@GDY with different voltages with diluted 10 times electrolyte.

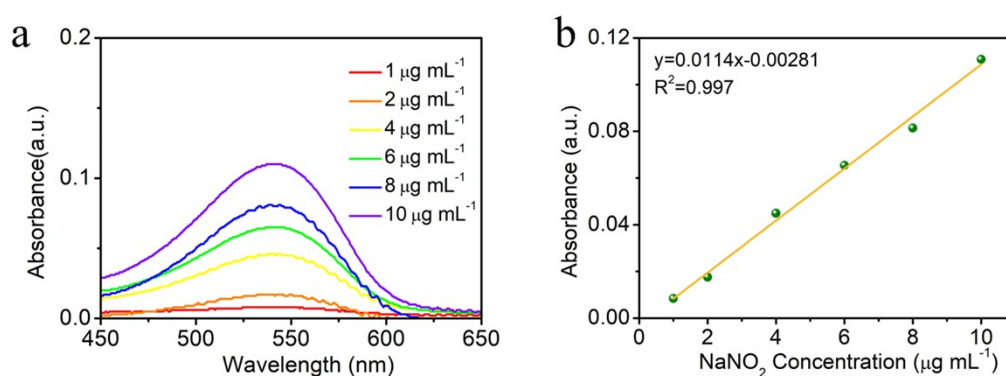


Figure S6. a) Absorption spectra of the solutions containing different known NO₂⁻ concentrations. b) The corresponding linear relationship between the absorbance at 540 nm and the NO₂⁻ concentration.

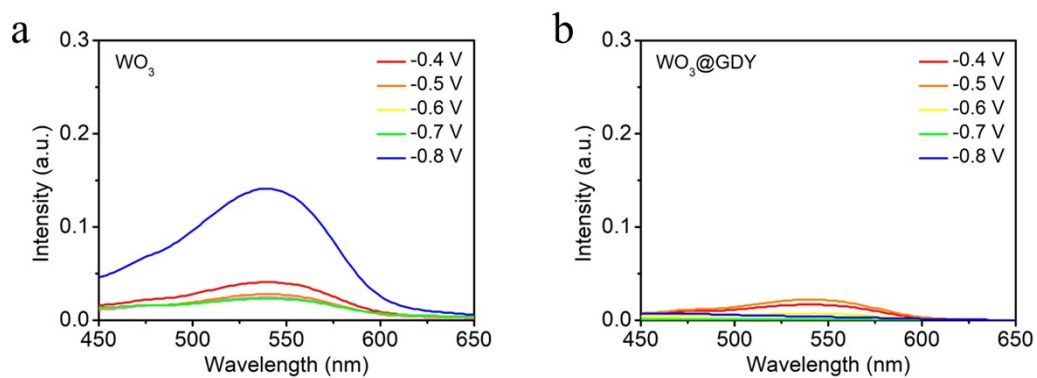


Figure S7. Absorption spectra of the electrolyte solutions at different potentials for detecting NO_2^- for a) WO_3 and b) $\text{WO}_3@\text{GDY}$.

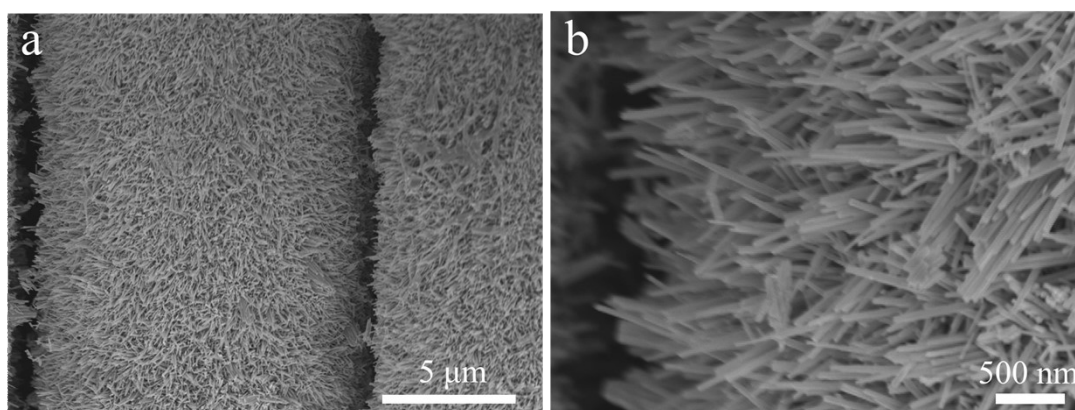


Figure S8. Low and high magnification SEM images of $\text{WO}_3@\text{GDY}$ after continuous electrolysis for 20 hours.

Table S1. Comparison of the electrocatalytic NtRR performance under acidic conditions.

Catalyst	$\text{FE}_{(\text{NH}_3)}$	$\text{Y}_{(\text{NH}_3)}$	Electrolyte	Ref.
$\text{WO}_3@\text{GDY}$	85.4	$2582.6 \mu\text{g h}^{-1} \text{cm}^{-2}$	0.1 M HCl+ 0.1 M KNO_3	This work
CuO	80	$162 \mu\text{mol cm}^{-2} \text{h}^{-1}$	0.05 M KNO_3 + 0.05 M H_2SO_4	1
Ti	82	-	0.1 M KNO_3 +0.3 M KNO_3	2

Ir NTs	84.7	921 $\mu\text{g h}^{-1} \text{mg}_{\text{cat}}^{-1}$	0.1 M HClO ₄ + 1 M NaNO ₃	3
Cu-PTCDA	8	485.7 $\mu\text{g h}^{-1} \text{mg}^{-1}$	0.001 M HCl + 0.5 g L ⁻¹ KNO ₃	4
PA-RhCu	93.7	2.40 $\text{mg h}^{-1} \text{mg}_{\text{cat}}^{-1}$	0.1 M HClO ₄ + 0.05 M KNO ₃ ¹	5

Reference

1. R. Daiyan, T. Tran-Phu, P. Kumar, K. Iputera, Z. Tong, J. Leverett, M. H. A. Khan, A. Asghar Esmailpour, A. Jalili, M. Lim, A. Tricoli, R.-S. Liu, X. Lu, E. Lovell and R. Amal, Nitrate reduction to ammonium: from CuO defect engineering to waste NO_x-to-NH₃ economic feasibility, *Energy & Environmental Science*, 2021, **14**, 3588-3598.
2. J. M. McEnaney, S. J. Blair, A. C. Nielander, J. A. Schwalbe, D. M. Koshy, M. Cargnello and T. F. Jaramillo, Electrolyte Engineering for Efficient Electrochemical Nitrate Reduction to Ammonia on a Titanium Electrode, *ACS Sustainable Chemistry & Engineering*, 2020, **8**, 2672-2681.
3. J.-Y. Zhu, Q. Xue, Y.-Y. Xue, Y. Ding, F.-M. Li, P. Jin, P. Chen and Y. Chen, Iridium Nanotubes as Bifunctional Electrocatalysts for Oxygen Evolution and Nitrate Reduction Reactions, *ACS Applied Materials & Interfaces*, 2020, **12**, 14064-14070.
4. G.-F. Chen, Y. Yuan, H. Jiang, S.-Y. Ren, L.-X. Ding, L. Ma, T. Wu, J. Lu and H. Wang, Electrochemical reduction of nitrate to ammonia via direct eight-electron transfer using a copper–molecular solid catalyst, *Nature Energy*, 2020, **5**, 605-613.
5. Z. X. Ge, T. J. Wang, Y. Ding, S. B. Yin, F. M. Li, P. Chen and Y. Chen, Interfacial Engineering Enhances the Electroactivity of Frame-Like Concave RhCu Bimetallic Nanocubes for Nitrate Reduction, *Advanced Energy Materials*, 2022, **12**, 2103916.